Effect of surface modes on photon traversal through stop bands of dielectric stacks

Natalia Malkova* and Garnett W. Bryant
Atomic Physics Division and Joint Quantum Institute, NIST, Gaithersburg, Maryland 20899, USA

Sergey Polyakov and Alan Migdall
Optical Technology Division and Joint Quantum Institute, NIST, Gaithersburg, Maryland 20899, USA

(Received 24 April 2009; revised manuscript received 10 July 2009; published 28 October 2009)

We investigate the Hartman saturation effect of photons traveling through barriers created by stop bands of multilayer stacks. We provide a theoretical basis for the recently observed drastic changes in photon transversal times due to adding a single layer. Using a comprehensive coupled mode analysis and rigorous transfer matrix approach, we show that the experimentally observed effect is caused by surface modes. We investigate the origin and properties of the surface modes and identify them as Tamm-type states.

DOI: 10.1103/PhysRevB.80.165127 PACS number(s): 78.68.+m, 42.65.Tg, 73.20.At, 42.79.Gn

I. INTRODUCTION

Precise control of photon propagation times through subwavelength dielectric structures is becoming increasingly important for many optics applications including optical quantum computing and nanophotonics. This is partly the reason why, after a remarkable theoretical prediction by MacColl[1] in 1932, effects related to propagation of a photon through opaque barriers have been revisited several times during the last decades.[2–4] The effect known as the Hartman effect[5] states that the time needed for a photon to pass through an opaque barrier asymptotically reaches a limit as thickness increases. In principle, this implies an apparent superluminal group velocity. This curious result has been verified at the single photon level in experiments performed on one-dimensional stop-band materials.[6,7] It was demonstrated that an electromagnetic pulse with its frequency centered in a stop band passes the barrier with a superluminal group velocity, without, however, contradicting causality.[3,8] Even more surprising results have been reported quite recently.[8–10] Stacks (i.e., one-dimensional photonic crystals) made of alternating quarter-wave layers H and L of high refractive index (n_H) and lower refractive index (n_L) with a substrate (index n_o) have been studied (see left panel of Fig. 1). It was shown that the single photon transversal times in the stop band of stacks with different terminations are significantly different. In some cases the group velocity changes by more than a factor of two, and can change from subluminal to apparently superluminal.

This effect was first predicted from numerical solutions of Maxwell equations.[8,9,11] In particular, it has been shown that light transversal times $\tau(\omega_o)$ at the frequency ω_o, corresponding to the middle of the first stop band, experiences discontinuous changes depending on the type of structures used. We reproduce this result in the right panel of Fig. 1. Throughout this paper, we normalize the transversal time by the inverse frequency of the center of the first stop band of the quarter-wave stack, ω_o. The dashed line indicates the luminal time, that is, the time required for the photon to tranverse the same distance in vacuum. Indeed, the saturation time with the number of paired layers N in the quarter-wave stacks depends strongly on which structure was used: $(HL)^N H$, $(HL)^N$, or $(LH)^N L$, as seen in the right panel of Fig. 1. When one layer is added to any structure, the structure type switches. For large N, the transversal time changes (jumps) between different curves for each structure type. Curiously, the large changes of transversal time may result in group velocities that range from superluminal to subluminal. Although this numerical result agrees with the experiment,[10] it does not provide any understanding for the underlying physics. In particular, one of the puzzling questions that remains unanswered is why the saturation transversal times (i.e., for $N \to \infty$) almost precisely satisfy the relation: $\tau_{(LH)^N L} - \tau_{(HL)^N H} = 2(\tau_{(LH)^N L} - \tau_{(LH)^N}) \equiv 2\Delta\tau$ as shown in Fig. 1.

In this contribution, we identify the physical mechanism behind this phenomenon, addressing specifically why the transversal times change in jumps with the addition of a single layer. Answering this question will allow a wider class of structures including two-dimensional and three-dimensional photonic crystals to be designed with specific transversal times. We investigate in detail the propagation of electromagnetic waves through stacks with different configurations. In particular, we analyze the dependence of transmittance and the density of modes (DOM) on the type of termi-

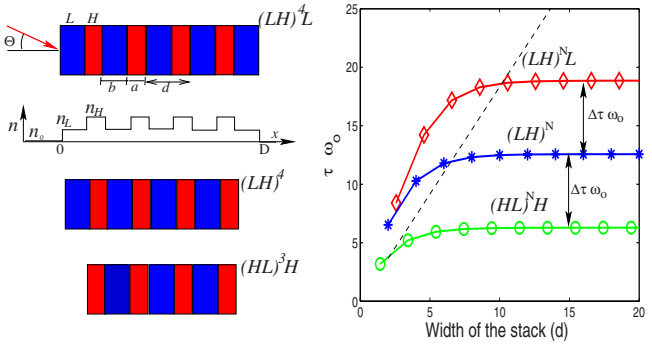

FIG. 1. (Color online) (left panel) Schematics of quarter-wave stacks $(LH)^4L$, $(LH)^4$, and $(HL)^3H$ studied with the corresponding refractive index profile. (right panel) Calculated normalized transversal times $\tau(\omega_o)\omega_o$ as a function of thickness of the quarter-wave stacks (in units of lattice period d) $(HL)^N H$ (circles), $(LH)^N$ (stars), and $(LH)^N L$ (diamonds), where $n_H=2$, $n_L=1.5$, and $n_o=1$. ω_o is the center of the first forbidden band of the quarter-wave stack. The solid lines are guides for the eyes. The dashed line indicates the luminal time.

nation of the structure, the number of layers, incident angle, and separation between the H layers. We apply a rigorous transfer matrix approach and comprehensive coupled mode theory to find modes of finite dielectric stacks that fall in the stop band. Our main finding is that the changes of the transversal times are caused by surface modes exactly in the middle of the stop band. The surface modes are supported in the structures terminated with the L layer (on at least one side). We present a comprehensive study of the origin and properties of the surface modes and identify them as Tamm-type surface modes known for solids.[12,13]

The surface modes in multilayer structures have been studied both in the regime of guided (localized) photonic modes[14,15] and in the regime of transmitted photonic resonances.[16] The analogy of surface modes in optics with surface states in solids has been pointed out by many groups[17–21] starting from Yariv's pioneering work.[14] However the temporal effects due to surface modes have not been previously considered. In this study we demonstrate that the existence of the surface modes leads to temporal optical anomalies. Moreover, in contrast to the general trend in the current literature[17,18,21] where surface modes are labeled as Tamm modes without definitive proof, we present a detailed analysis which proves that the modes we are dealing with are indeed Tamm modes. The formalism presented here can be useful for a better understanding of the effects in more complex optical structures and propagation by transmission and guiding.

The paper is organized as follows. In Sec. II, using the calculated DOM, we analyze the electromagnetic spectra for different structures. Based on this analysis we present the evidence for surface modes. In Sec. III, we discuss the evolution of the electromagnetic spectrum when varying the separation between the H layers. This analysis explains the origin of the surface modes. Summary and outlook are given in Sec. IV.

II. ELECTROMAGNETIC SPECTRUM OF QUARTER-WAVE STACKS: EVIDENCE OF THE SURFACE MODES

We study the stacks sketched in the left panel of Fig. 1. We first focus on quarter-wave stacks because these are the structures which have been extensively studied.[8–11] For quarter-wave stacks $an_H=bn_L$, where a and b are the thicknesses of the H and L layers, respectively, while $n_{H,L}$ are the corresponding refractive indexes. The period of these structures is given by $d=a(1+n_H/n_L)$, and the center of the first forbidden band is $\omega_o=\frac{\pi c}{a(1+n_H/n_L)}$. For numerical modeling, we assume, $n_H=2$ and $n_L=1.5$. For simplicity, we consider stacks that terminate directly to air, i.e., there is no substrate on either side, $n_o=1$. We focus on TE wave propagation.

We are interested in the electromagnetic spectrum of different stacks. The spectrum of the infinite, periodic structure consists of continuous allowed (pass) and forbidden (stop) bands, that are completely defined by the dielectric constants and widths of the alternating layers.[14] The spectrum of a finite structure manifests itself through the peaks of the DOM, $\rho(\omega)$. The DOM for an arbitrary one-dimensional index profile $n(x)$, can be evaluated from the complex transmission coefficient $t(\omega)=t_{real}(\omega)+it_{imag}(\omega)$ (Ref. 22) as

$$\rho(\omega)=\frac{1}{D}\frac{t'_{imag}t_{real}-t'_{real}t_{imag}}{t^2_{real}+t^2_{imag}}. \quad (1)$$

Here prime stands for the derivative with respect to ω and D is the thickness of the structure. Using a standard transfer matrix approach[14] we calculate $t(\omega)$ and evaluate the DOM from Eq. (1). The transmission coefficient $|t(\omega)|$ (dashed curves) and DOM $\rho(\omega)$ (solid curves) for normal and oblique ($\Theta=74°$) incidences are shown in Fig. 2.

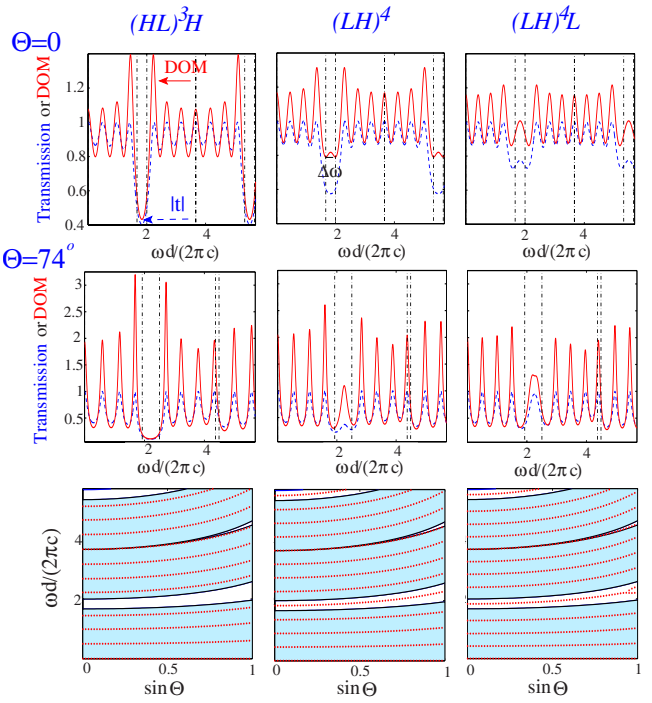

FIG. 2. (Color online) The transmission coefficient $|t(\omega)|$ (dashed curves) and DOM $\rho(\omega)$ (solid curves) for normal and oblique ($\Theta=74°$) incidence are shown in the top and middle rows, respectively. The vertical dash-dotted lines indicate the band edges of an infinite stack. The bottom row shows the dispersion of the electromagnetic modes as a function of incident angle Θ. The shaded areas mark the allowed bands of an infinite stack, the dots show the modes of the finite stack. The left, middle, and right panels correspond to the stacks $(HL)^3H$, $(HL)^4$, and $L(HL)^4$, respectively.

From Fig. 2 we note that adding one or two L layers on the sides of the structures changes the DOM drastically. There is no peak inside the forbidden band of the $(HL)^3H$ structure, either for normal or oblique incidence. However, adding one L layer to make the $(HL)^4$ structure, results in a peak in the middle of the forbidden band (top row, middle panel of Fig. 2). This peak is visible in the DOM spectrum for normal incidence, but is not apparent in the transmission spectrum. The peak becomes better defined for oblique incidence, when it can also be seen in the transmission spectrum (middle row, middle panel of Fig. 2). When another L layer is added, the resulting structure, $L(HL)^4L$, exhibits a noticeable peak inside the forbidden band in the transmission spectrum under the normal incidence (top row, right panel of Fig.

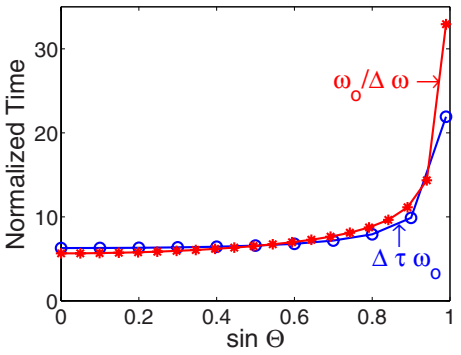

FIG. 3. (Color online) The normalized lifetime of the surface mode $\omega_o/\Delta\omega$ (stars) and the normalized jump of transversal time $\Delta\tau(\omega_o)\omega_o$ (circles) calculated as a function of incident angle.

2). This peak is even more pronounced in the DOM. Importantly, this peak is resolved into two peaks under oblique incidence, as evidenced in the middle row of the right panel of Fig. 2, which suggests that these are two separate modes inside this forbidden band.

We summarize our results in the bottom row of Fig. 2 where the spectrum of the electromagnetic modes versus the sine of incident angle Θ are shown. In this figure the allowed bands of the infinite stacks are shaded, while the eigenmodes of finite stacks are shown by dots. We see that all modes for the $(HL)^3H$ structure fall inside the allowed bands (bottom row, left panel of Fig. 2), while there are one or two modes for the $(LH)^4$ (bottom row, middle panel of Fig. 2) and $(LH)^4L$ (bottom row, right panel of Fig. 2) stacks inside the forbidden bands. Modes appear inside the forbidden band, when there are structural defects. For the structures studied here, these defects can only be due to structure termination, as confirmed by the field distribution of the gap modes localized near the surface layer. The existence of surface modes in the forbidden band coincides with the increasing transversal times. The relation $\tau_{(HL)^NH} < \tau_{(HL)^N} < \tau_{(LH)^NL}$, for large N, observed in Fig. 1, is explained if the photons are trapped by the one (two) surface states in the $(LH)^N$ $[(LH)^NL]$ stack, while the photons propagate freely through the $(HL)^NH$ stack. Moreover, one could suspect that the above-mentioned relation $\tau_{(LH)^NL} - \tau_{(HL)^NH} = 2(\tau_{(LH)^NL} - \tau_{(LH)^N})$ is due to photon trapping that is twice as long for the two surface modes of the $(LH)^NL$ stack than for the one surface mode of the $(LH)^N$ stack. To establish this conjecture, we consider the relation between the value of $\Delta\tau$ and the lifetime of the surface mode. We can evaluate the lifetime of the surface mode as the inverse of the half width at half maximum (HWHM) of the relevant resonant peak of the DOM, $1/\Delta\omega$ (see top row of Fig. 2). We can independently find the transversal time as $\tau(\omega) = D\rho(\omega)$.[22] In Fig. 3 we compare the values of $\Delta\tau(\omega_o)\omega_o$ (circles) and $\omega_o/\Delta\omega$ (stars) calculated for different incident angles. Our results demonstrate a good agreement between $\Delta\tau(\omega_o)$ and $1/\Delta\omega$ for all values of the angle of incidence. This is a direct signature of surface modes because the jumps in the saturated values of the transversal times are almost exactly equal to the surface mode lifetimes. Also, we notice that $\Delta\tau(\omega_o)$ drastically increases with increasing incident angle. This effect follows directly from the properties of surface modes studied above. Indeed when comparing Figs. 2(a) and 2(b), we noticed that a surface mode becomes better defined, and the two modes are resolved in the stack $(LH)^4L$, with increasing angle of incidence when approaching the guided mode regime.[16] This implies a decrease in the surface mode HWHM, and a corresponding increase in the photon trapping time by the surface mode.

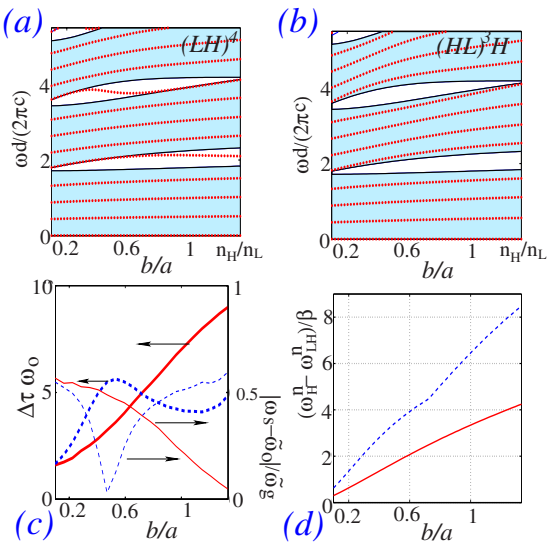

FIG. 4. (Color online) The change of the electromagnetic spectrum calculated at $\sin\Theta = 0.8$ versus the ratio b/a for the structures (a) $(HL)^4$, that exhibits surface modes and (b) $(HL)^3H$, that does not exhibit surface modes; (c) $\Delta\tau\omega_o$ calculated at the central frequency of the first (bold solid curve) and second (bold dashed curve) forbidden bands as a function of b/a. Thin solid and dashed curves show the normalized detuning of the surface modes, $|\omega_s - \tilde{\omega}_o|/\tilde{\omega}_g$, inside the first and second forbidden bands, respectively. Here $\tilde{\omega}_o$ is the central frequency of the relevant forbidden band with width $\tilde{\omega}_g$, ω_o is the center of the first forbidden band of the quarter-wave stack. (d) The value of $|\omega_H^n - \omega_{LH}^n|/\beta$ at $n=1$ (solid curve) and 2 (dashed curve) as a function of b/a.

III. ORIGIN OF THE SURFACE MODES

We have established that the jumps in the transversal times for different quarter-wave structures is due to surface mode effects. Now, we would like to understand surface mode formation in dielectric stacks: in particular, why terminating a structure with an L layer leads to a surface mode, whereas termination on an H layer does not. Also, why does the surface mode in quarter-wave stacks lies precisely in the middle of the forbidden band? To answer these questions, we trace the evolution of the electromagnetic spectrum when varying the thickness of the L layers in the interval $b = [0.1, n_H/n_L]a$, while keeping a constant. Note that this class of structures is larger than the class of quarter-wave structures. The corresponding quarter-wave structure for this class is $b = an_H/n_L$. In Figs. 4(a) and 4(b) we show the change of the electromagnetic spectrum calculated at $\sin\Theta = 0.8$ versus the ratio b/a for the structures $(HL)^4$ and $(HL)^3H$. We see that no mode falls in the forbidden bands of

the $(HL)^3H$ stacks [Fig. 4(b)], for any value of b/a. On the other hand, in the stacks $(HL)^4$, surface modes are present both in the first and the second forbidden bands [Fig. 4(a)]. However, their frequencies change as a function of b/a. For low values of b/a one mode resides on the edge of the first forbidden band, and falls into the first forbidden band for $b/a \sim 0.3$. It forms the surface mode which gradually moves to the middle of the forbidden band when approaching $b/a=n_H/n_L$ for a quarter-wave stack. At the same time, the mode inside the second forbidden band crosses the gap and merges with the allowed band at $b/a>0.8$. In Fig. 4(c) we present the normalized difference in saturation values of transversal times, $\Delta\tau\omega_o$, calculated for the central frequency $\tilde{\omega}_o$ of the first (bold solid curve) and second (bold dashed curve) forbidden bands as a function of b/a. Note that as before we normalize transversal times by a constant ω_o, the central frequency of the first forbidden band of the quarter-wave stack independent of the varying ratio b/a. We compare these results with the normalized detuning of the surface mode from the central frequency of the relevant forbidden bands, $|\omega_s-\tilde{\omega}_o|/\tilde{\omega}_g$, where $\tilde{\omega}_g$ is the width of the relevant forbidden band. We see that indeed the difference between transversal-time saturation values $\Delta\tau$ reaches its maximum when the frequency of light at the center of the forbidden band coincides with that of the surface mode, $|\omega_s-\tilde{\omega}_o|\to 0$. The same conclusion can be also drawn from the measurements of $\Delta\tau$ as a function of the detuning of the probe frequency from ω_o.[10]

We now present a comprehensive explanation of the origin of the surface modes in terms of the coupled mode theory developed for Tamm surface states in photonic crystals.[19,20] We represent the stack $(HL)^{N-1}H$ as N H layers coupled through the L layers. The resonant spectrum of each H layer is defined by $\omega_H^n=\pi nc/(n_Ha)$ (where n is an integer number), which is independent of whether the layer is embedded in air or in a medium of refractive index n_L. Because of this, each H layer of the stack including the end layers can be viewed as identical. The coupling between N layers must split each of the resonant modes into N modes. Since all H layers are identical and they are connected by the identical L layers, these modes will fill allowed bands only. No mode can fall into the forbidden bands.[19] However, adding one L layer to the interface, as it is done in the $(LH)^N$ stack, changes the eigenfrequency of one of the end H layers to $\omega_{LH}^n=\pi nc/(n_Lb+n_Ha)$. Note that for the quarter-wave stack $\omega_{LH}^n=\omega_H^n/2$. According to the theory of Tamm states,[12,13] the condition for the surface state to appear is the asymmetry in the surface cell (layer), that is $|\omega_H^n-\omega_{LH}^n|>\beta$, where β is the coupling constant, which can be estimated as a quarter of the width of the allowed band.[13,20] In the case of strong asymmetry in the surface cell, $|\omega_H^n-\omega_{LH}^n|/\beta \gg 1$, the frequency of the surface mode is equal to the resonant frequency of the surface layer. In Fig. 4(d) we show the calculated value of $|\omega_H^n-\omega_{LH}^n|/\beta$ as a function of b/a for the first two bands $(n=1,2)$. We see that $|\omega_H^n-\omega_{LH}^n|/\beta$ becomes larger than 1 at $b/a>0.3(0.15)$ for $n=1(2)$. This indicates the asymmetry in the surface layer that supports Tamm modes. These conditions coincide with appearance of the surface modes in the stack $(LH)^4$, calculated directly, see Fig. 4(a). Moreover, we can see in Fig. 4(d) that for the quarter-wave stack (i.e., at $b/a=n_H/n_L$) the asymmetry in the surface layer is rather strong. Therefore, the frequency of the surface mode must be close to ω_{LH}^n, corresponding to the middle of the first forbidden band at $n=1$, ω_o. This explains the appearance of the surface mode exactly in the middle of the forbidden band of the quarter-wave stack shown in Fig. 4(a).[23] In case of the stack $(LH)^NL$ terminated on both sides by the L layers, each of the end layers will produce an identical surface mode. Because surface modes couple to one another, these modes split, as evidenced in Fig. 2(c). Note that the thinner the stack is (or the smaller N) the larger the splitting is.

In summary the origin of the surface modes in the class of stacks with $b=[0.1,n_H/n_L]a$ is governed by the following: (1) with increasing b/a the asymmetry in the surface layer (whose large value is indicative of the Tamm states) increases [Fig. 4(d)]; (2) the surface mode frequency approaches the center of the forbidden band [thin curves in Fig. 4(c), right vertical axis]; and (3) the lifetime of the surface mode, that is responsible for long delays in photon transversal times, increases [thick curves in Fig. 4(c), left vertical axis]. This analysis allows us to understand the origin of the surface modes in the structures studied and gives direct evidence for the Tamm-type character of these modes.

An extension of the presented analysis to the case of the stacks terminated by a substrate shows that the appearance of surface modes strongly depends on the choice of the substrate. This is consistent with the previously published results.[16] The effect of the substrate on the transversal times was also observed experimentally.[10]

IV. SUMMARY AND OUTLOOK

We have analyzed light propagation through stop bands in three types of stacks which differ by the end layers. We have shown that the strong difference in the transversal times is due to the surface modes. Our analysis proves that the surface modes delay photons propagating through the dielectric band gap, increasing their transversal time. We demonstrate that the existence of surface modes is warranted by the strong asymmetry in the surface layer. Hence, we identify these modes as Tamm-type states. We demonstrated that the surface modes are sensitive to the details of the structure such as the choice of the terminating layer and separation between layers. We have shown that the lifetime of Tamm states is directly related to the detuning from the center of the stop band. In particular, our results predict an interesting opportunity for controlling the transversal times through the structure $(HL)^N$ by changing the width and/or refractive index of the L layers. The basic and intuitive approach of our study offers a powerful tool for the design of more complex subwavelength structures with propagation properties tailored to specific applications.

*nmalkova@nist.gov

[1] L. A. MacColl, Phys. Rev. **40**, 621 (1932).
[2] M. Buttiker and R. Landauer, Phys. Rev. Lett. **49**, 1739 (1982).
[3] M. D. Stenner, D. J. Gauthler, and M. Nelfeld, Nature (London) **425**, 695 (2003).
[4] G. Nimtz, IEEE J. Sel. Top. Quantum Electron. **9**, 79 (2003).
[5] T. E. Hartman, J. Appl. Phys. **33**, 3427 (1962).
[6] A. M. Steinberg, P. G. Kwiat, and R. Y. Chiao, Phys. Rev. Lett. **71**, 708 (1993).
[7] Ch. Spielmann, R. Szipocs, A. Stingl, and F. Krausz, Phys. Rev. Lett. **73**, 2308 (1994).
[8] V. Laude and P. Tournois, J. Opt. Soc. Am. B **16**, 194 (1999).
[9] D. R. Solli, J. J. Morehead, C. F. McCormick, and J. M. Hickmann, J. Opt. A, Pure Appl. Opt. **10**, 075204 (2008).
[10] N. Rutter, S. Polyakov, P. Lett, and A. Migdall, Proceedings of the CLEO/IQEC-09, 2009; N. Rutter, S. Polyakov, P. Lett, and A. Migdall (unpublished).
[11] J. P. Dowling, IEE Proc.: Optoelectron. **145**, 420 (1998).
[12] I. E. Tamm, Phys. Z. Sowjetunion **1**, 733 (1932); Z. Phys. **76**, 849 (1932).
[13] A. Many, Y. Goldstein, and N. B. Grover, *Semiconductor Surfaces* (North-Holland, Amsterdam, 1965).
[14] P. Yeh, A. Yariv, and C.-S. Hong, J. Opt. Soc. Am. **67**, 423 (1977).
[15] P. Yeh, A. Yariv, and A. Y. Cho, Appl. Phys. Lett. **32**, 104 (1978).
[16] M. L. H. Lahlaouti, A. Akjouj, B. Djafari-Rouhani, and L. Dobrzynski, Phys. Rev. B **61**, 2059 (2000).
[17] K. G. Makris, S. Suntsov, D. N. Christodoulides, G. I. Stegeman, and A. Hache, Opt. Lett. **30**, 2466 (2005).
[18] C. R. Rosberg, D. N. Neshev, W. Krolikowski, A. Mitchell, R. A. Vicencio, M. I. Molina, and Y. S. Kivshar, Phys. Rev. Lett. **97**, 083901 (2006).
[19] N. Malkova and C. Z. Ning, Phys. Rev. B **73**, 113113 (2006).
[20] N. Malkova and C. Z. Ning, J. Phys.: Condens. Matter **19**, 056004 (2007).
[21] M. I. Molina, R. A. Vicencio, and Y. S. Kivshar, Opt. Lett. **31**, 1693 (2006).
[22] J. M. Bendickson, J. P. Dowling, and M. Scalora, Phys. Rev. E **53**, 4107 (1996).
[23] However, this analysis is limited to the case of the one-band spectra (Ref. 13). Because of this, it fails for the surface mode inside the second band gap at $b/a>0.8$, when moving down in frequency, the mode meets the second allowed band.